

# Eddy Current Influences on the Dynamic Behaviour of Magnetic Suspension Systems

Colin P. Britcher<sup>†</sup>, Dale V. Bloodgood<sup>‡</sup>  
Department of Aerospace Engineering  
Old Dominion University

## Abstract

This report will summarize some results from a multi-year research effort at NASA Langley Research Center aimed at the development of an improved capability for practical modelling of eddy current effects in magnetic suspension systems. Particular attention is paid to large-gap systems, although generic results applicable to both large-gap and small-gap systems are presented. It is shown that eddy currents can significantly affect the dynamic behaviour of magnetic suspension systems, but that these effects can be amenable to modelling and measurement. Theoretical frameworks are presented, together with comparisons of computed and experimental data particularly related to the Large Angle Magnetic Suspension Test Fixture at NASA Langley Research Center, and the Annular Suspension and Pointing System at Old Dominion University. In both cases, practical computations are capable of providing reasonable estimates of important performance-related parameters. The most difficult case is seen to be that of eddy currents in highly permeable material, due to the low skin depths. Problems associated with specification of material properties and areas for future research are discussed.

## Background

Whenever a time-varying magnetic flux penetrates a conducting medium, eddy-currents will be generated according to a simple application of Faraday's Law of Induction :

$$\nabla \times \vec{E} + \frac{\partial \vec{B}}{\partial t} = 0 \quad (1)$$

or alternatively :

$$V = N \frac{d\phi}{dt} \quad (2)$$

- where  $E$  represents the electric field,  $B$  magnetic flux density,  $V$  electric potential,  $N$  the number of turns in a coil, and  $\phi$  magnetic flux. Two fundamental effects must be considered for a proper understanding of eddy current behaviour, particularly in large-gap suspension systems. These are first, the reactive coupling from the magnetic fluxes required for suspension purposes to the eddy current circuits and second, the resistive dissipation in those circuits. The former effect is the driving term, the second clearly the

---

<sup>†</sup> Associate Professor of Aerospace Engineering

<sup>‡</sup> Graduate Research Assistant

dissipative term. Further, the signs of terms in equation 1 suggest exclusion (or cancellation) of flux from the eddy current circuits; normally known as Lenz's Law.

Important insight can be gained from consideration of a simple model, resembling a single-turn transformer, with the eddy current circuit being the secondary. The general form of the results are easily shown to be [1] :

$$I_e = I \left( \frac{-L_m s}{R_e + L_e s} \right) \quad (3)$$

- where  $I, I_e$  are the driven coil and eddy currents respectively,  $R_e, L_e, L_m$  are the resistance, self-inductance and mutual-inductance of the eddy current circuit. If the field component  $B_j$  at some location due to a unit current in the primary coil is given by  $K_j$  and the corresponding field component due to the eddy current is given by  $K_{e_j}$  then :

$$B_j = K_j I + K_{e_j} I_e = \left( 1 - \frac{K_{e_j} L_m s}{K_j (R_e + L_e s)} \right) \quad (4)$$

The basic behaviour is illustrated in Figure 1, and is seen to be a roll-off in the magnitude of the useful field, with a phase lag peaking at some "resonant" frequency, then asymptoting to zero phase at high frequency. The frequency of resonance and the magnitude of the peak phase shift (or maximum attenuation) are clearly of great interest. It has previously been shown that order of magnitude estimates can be made for simple geometries using standard formulae for single-turn coils and the like [1].

A number of large-gap geometries have been studied and experimental evidence supports the form of equations 3 and 4. Some of these results will be reviewed later in this paper. In the meantime, certain practical difficulties that have been experienced in developing mathematical models will be discussed. The "resonant frequency", or frequency of maximum phase lag from equations 3 or 4, and the maximum phase lag are easily shown to be [1] :

$$\omega_{\phi_{max}} = \sqrt{\frac{R_e^2}{L_e^2 - L_m L_e}} \quad ; \quad \phi_{max} = \text{Tan}^{-1} \left( \frac{L_m}{2\sqrt{L_e^2 - L_m L_e}} \right) \quad (5)$$

In the former case, the resistance of the eddy current circuit must be known. One would be forgiven for thinking that estimation of eddy current circuit resistance was a simple matter of inserting material resistivity into simple geometric formulae. This apparently trivial step quickly becomes a significant challenge, when it is realized that the resistivity of common engineering metals varies greatly between different alloys, as illustrated in Table 1, and is often also a function of heat treatment and cold work. Further, any welded, bolted or riveted joints present unknown and practically unmeasurable properties.

Where the "skin depth" or penetration depth of the eddy currents is frequency dependent, modified models are required. Careful consideration of the physics of the problem and

Table 1 - Resistivity of Aluminum Alloys [2]

Type	Resistivity, $\Omega\text{m} \times 10^{-8}$
Pure aluminum	2.65
2024-T0	3.4
2024-T3,4	5.7
5083	5.9
6061-T6	4.0

study of classical solutions assists in the formation of suitable models. Exact solutions for eddy currents in certain simplified geometries, such as infinite plates or bars are available [3,4]. The solution to the infinite plate problem, illustrated in Figure 2, is reproduced here for reference. The governing equation is the one-dimensional diffusion equation :

$$\frac{\partial^2 B_z}{\partial y^2} = \sigma \mu_o \mu_r \frac{\partial B_z}{\partial t} \quad (6)$$

- where  $\sigma$  is the material conductivity and can be solved for the geometry given in Figure 2, to give the total magnetic flux across the conductor as :

$$B_{total} = \frac{2}{\alpha} B_{surface} \text{Tanh}(\alpha b) \quad (7)$$

- where,  $\delta$  being the skin depth :

$$\alpha = \sqrt{j\omega\sigma\mu_o\mu_r} = \frac{1+j}{\delta} \quad (8)$$

The behaviour of equation 7 is rather unusual, suggesting that the total flux "rolls-off" at a rate of 10db/decade with a limiting phase lag of 45°. These are exactly half the corresponding values of a simple first-order pole. Similar results have been reported by other authors in small-gap applications [5] and the term "half-order pole" invoked. The term "fractional derivative" is found in materials science and structural dynamics literature, where similar temporal or spatial variations of physical properties have been noticed, albeit in different circumstances [6,7].

This result suggests an ad-hoc adjustment of equation 3 or 4, by a multiplier of the form :

$$\left( \sqrt{\frac{1}{1+\tau s}} \right) \quad (9)$$

- where  $\tau$  is based on the frequency where the skin depth becomes roughly equal to the effective material thickness. Reference 5 suggests an alternative form, based on an approximate analysis, where the denominator would take the form  $(1 + \sqrt{\tau s})$ . However, the form given in equation 9 is recommended here as being more consistent with other literature. The response predicted by equation 9, illustrated in Figure 3, shows broad correlation with observed behaviours. It should be noted that the integration of equation 9

into equation 3 and 4 requires some care. Where an electromagnet coil is closely coupled to an iron core, the flux penetration into the core, hence its magnetization, would lag according to equation 9. Where currents are being excited in non-magnetic, conducting media the situation is more complex. The flux penetration into the conductor will lag the driving field, suggesting a lag in the eddy current, but it should be noted that the driving field is itself strongly modified in the region of the conductor during the flux penetration process. Further analysis is required in this area. The remainder of this paper will review some experimental and computational results related to actual suspension and levitation systems.

### **Practical Examples**

Three suspension systems have been used during the course of this work for experimental evaluation of eddy current effects. Each system, together with representative experimental and computational results will now be briefly introduced. Experimental data relies on direct flux measurements with a Hall probe; computational results employ the finite element computer code ELEKTRA [10]

#### The Large-Angle Magnetic Suspension Test Fixture

The Large Angle Magnetic Suspension Test Fixture (LAMSTF) is a laboratory-scale levitation device comprising five conventional electromagnets arranged in a circular configuration, levitating a small suspended element containing a cylindrical permanent magnet core. The core is magnetized along the long axis of the cylinder, which in turn is horizontal. The suspended element can be controlled in five degrees of freedom [8,9]. Figure 4 shows the original layout of the system. The aluminum sensor frame and baseplate are worthy of note.

When LAMSTF was first commissioned, a discrepancy was discovered in the dynamic model, mainly manifested in the "pitch" degree-of-freedom (rotation of the suspended element about a lateral, horizontal axis). Extensive computations and measurements of the effects of eddy currents in the metallic support plate and position sensor structure indicated that the problem was mainly due to eddy currents induced in parts of the sensor structure. In fact, later replacement of this structure and the mounting plate with non-conducting material removed the discrepancy in the dynamic behaviour.

Many results have been previously published [1], but Figure 5 summarizes some important results.

#### The 6DOF-8C/2L system

A variety of "planar array" magnetic configurations were studied with the objective of developing a LAMSTF-like system with 6 degree-of-freedom control. The naming convention indicates that the system developed indeed achieves six degree-of-freedom

control (6DOF) by using eight control coils (8C) and two D.C. coils providing a background "levitation" field (2L). This configuration, illustrated in Figure 6, is far from the only possibility. The system was developed with the minimum of metallic structure (although iron cores are used in the eight control electromagnets), so the dynamic model proved to be quite reliable. However, a much larger system of a comparable configuration, the Large-Gap Magnetic Suspension System, is currently being developed at NASA Langley [11], where the levitation coils will be low-temperature superconductors. Eddy currents in the walls of the aluminum helium/nitrogen dewars containing these electromagnets were a real concern. The 6DOF-8C/2L system has therefore been used for a variety of verification experiments, repeating and extending work previously carried out with LAMSTF.

Figure 7 shows measured and computed results from the 6DOF-8C/L2 system for the case where a thin aluminum plate is placed between the control coils and the suspended element. Agreement is considered reasonable, despite some uncertainty in the resistivity of the actual aluminum alloy used. Readers are encouraged to compare the form of the responses in Figure 7 with the trends shown in Figure 3.

#### The Annular Suspension and Pointing System

The Annular Suspension and Pointing System (ASPS), shown in Figure 8, is a sophisticated prototype of a payload pointing and vibration isolation system for space payloads [12,13]. It comprises an annular iron rotor, suspended and controlled in six degrees-of-freedom by five magnetic bearing assemblies and one bidirectional linear motor. There is interest in developing advanced systems of similar configuration, so the existing hardware is being used to study modelling and control techniques. The achievable bandwidth of the magnetic bearings is of interest, either as a prerequisite to provision of higher system bandwidths, or to permit effective application of more sophisticated controller design techniques.

Computational modelling of the ASPS bearing stations has been attempted, albeit with some difficulties caused by the highly permeable iron cores used. This presents computational difficulties at the iron-air interface, particularly during the eddy current computations, as well as problems in specifying precise material properties. Nevertheless, it is clear that fluctuating coil currents provoke heavily damped flux waves propagating inwards through the iron electromagnet cores. This is the expectation from classical analysis, such as that presented earlier for the flat plate case, and can be captured in computations, as illustrated in Figure 9.

### **Discussion and Conclusions**

It has been shown that significant attenuation and phase shift of unsteady magnetic fields can occur in magnetic suspension and levitation systems. Accurate predictions are necessary for controller design purposes, as is a simple linear model. It has been shown

that simple models can be developed, albeit with an awkward "fractional derivative" term. Further research in this latter area is warranted.

### Acknowledgements

This work was supported by NASA Langley Research Center under Grant NAG-1-1056 and Cooperative Agreement NCC-1-248. The Technical Monitor was Nelson J. Groom of the Guidance and Control Branch.

### References

1. Britcher, C.P.; Foster, L.: Modelling of eddy currents related to the large angle Magnetic Suspension Test Fixture. 2nd International Symposium on Magnetic Suspension Technology, Seattle, WA, August 1995. NASA CP-3247.
2. Solid State Physics - Nonferrous Metals.
3. Stoll, R.L.: The Analysis of Eddy Currents, Clarendon, 1974.
4. Smythe, W.R.: Static and Dynamic Electricity, 3rd edition, McGraw-Hill, 1967.
5. Feeley, J.J.: A simple dynamic model for eddy currents in a magnetic actuator. IEEE Transactions on Magnetics, March 1996.
6. Torvik, P.J.; Bagley, R.L.: On the appearance of fractional derivatives in the behaviour of real materials. ASME Journal of Applied Mechanics, 1994.
7. Rossikhin, Y.A.; Shitikova, M.V.: Applications of fractional calculus to dynamic problems of linear and nonlinear hereditary mechanics of solids. Applied Mechanics Reviews, January 1997.
8. Britcher, C.P.; Ghofrani, M.; Britton, T.C.; Groom, N.J.: The large-angle magnetic suspension test fixture. International Symposium on Magnetic Suspension Technology, Hampton, VA, August 1991. NASA CP-3152.
9. Britcher, C.P.; Ghofrani, M.: A magnetic suspension system with a large angular range. Review of Scientific Instruments, July 1993.
10. Vector Fields Incorporated. ELEKTRA Reference Manual.
11. Groom, N.J.: Description of the Large Gap Magnetic Suspension Ground-Based Experiment. Technology 2000, published as NASA CP-3109, V.2, 1991
12. Cunningham, D.C. et. al.: Design of the annular suspension and pointing system. NASA CR-3343, October 1980.
13. Britcher, C.P.; Groom, N.J.: Current and future development of the annular suspension and pointing system. 4th International Symposium on Magnetic Bearings, Zurich, August 1994.

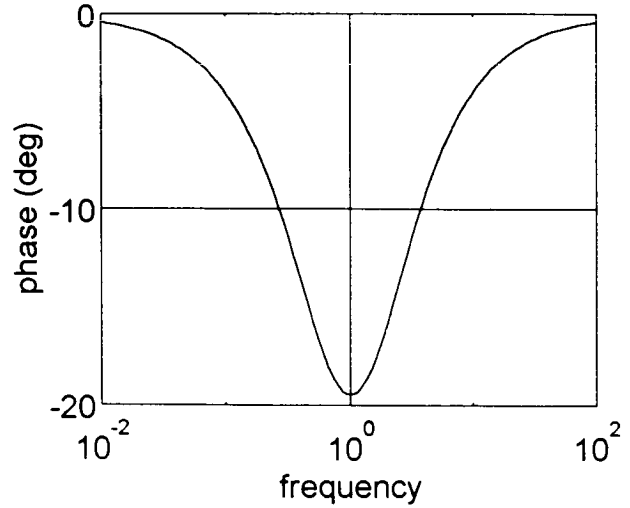
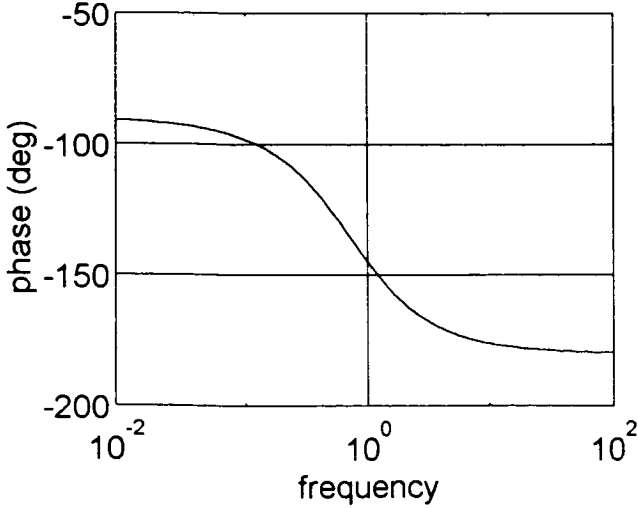
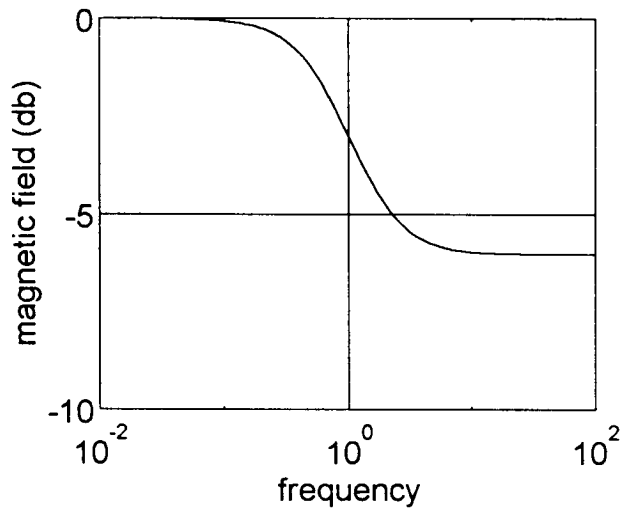
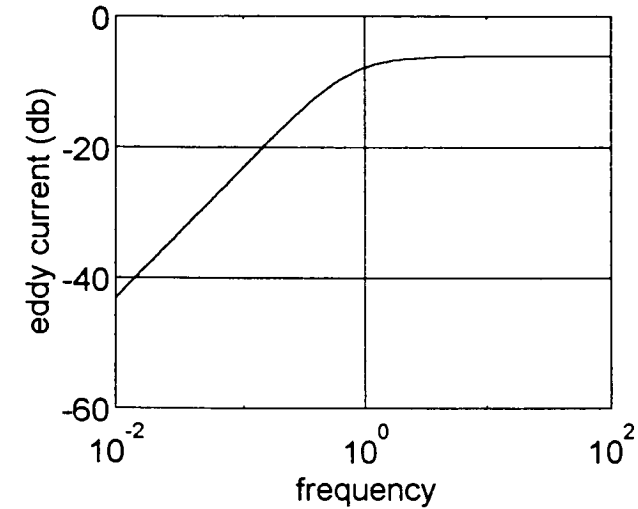
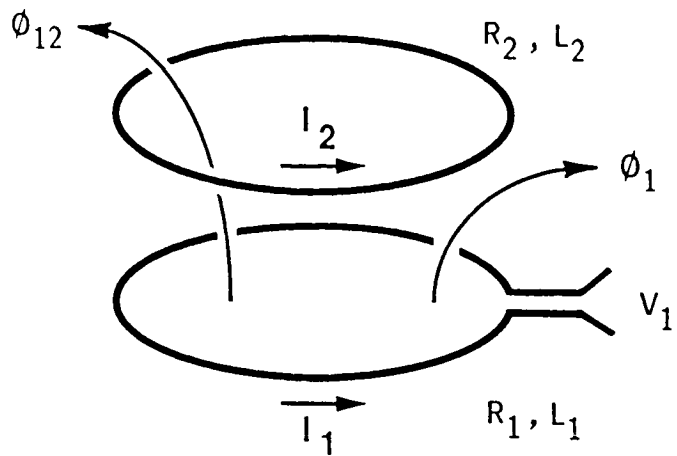


**Figure 1 - Transformer Model and Predicted Response**  
 Reasonant frequency adjusted to 1 unit, low/high frequency amplitude ratio = 0.5

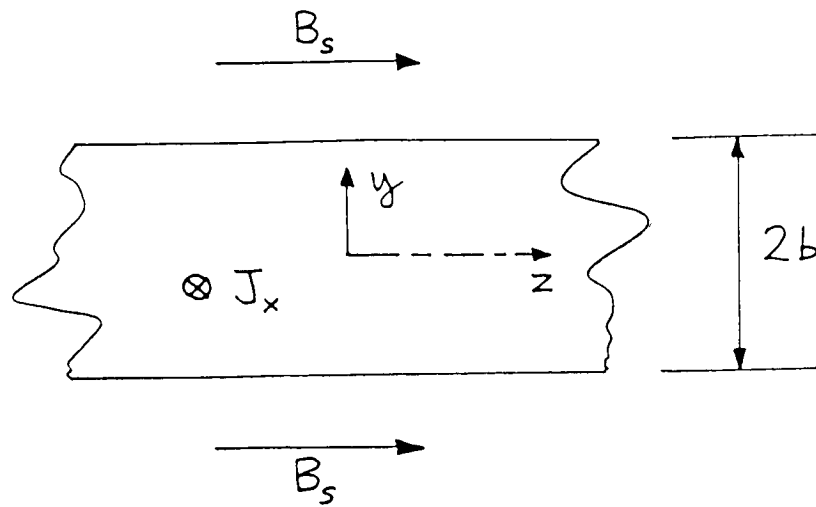


**Figure 2 - Eddy Currents in an Infinite Flat Plate**  
Description of geometry

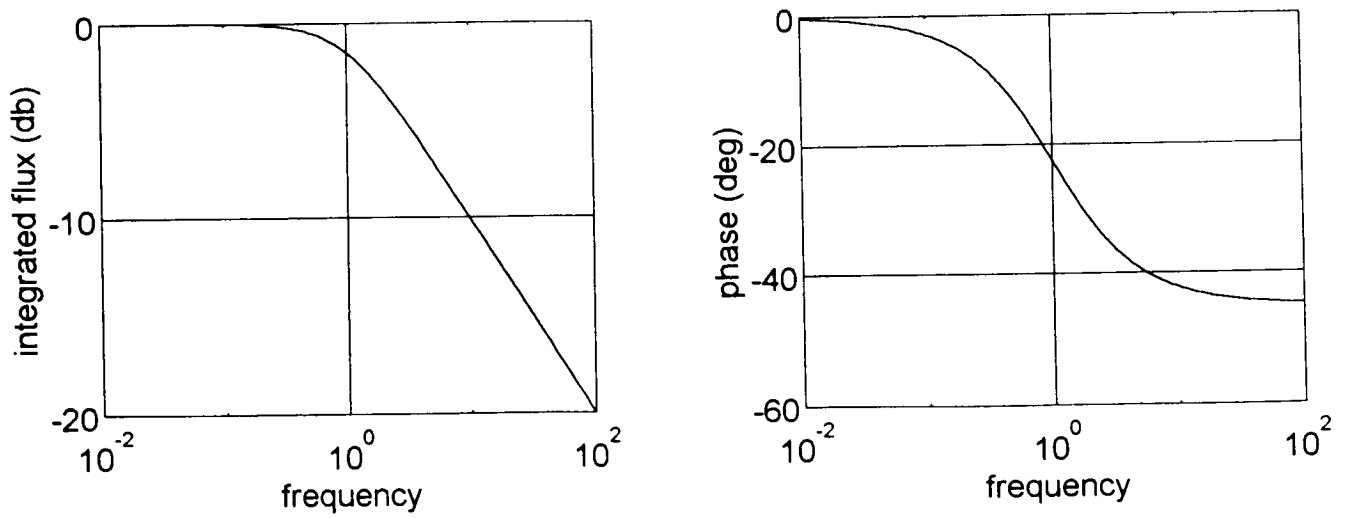


**Figure 3 - Response of Half-Order Pole**



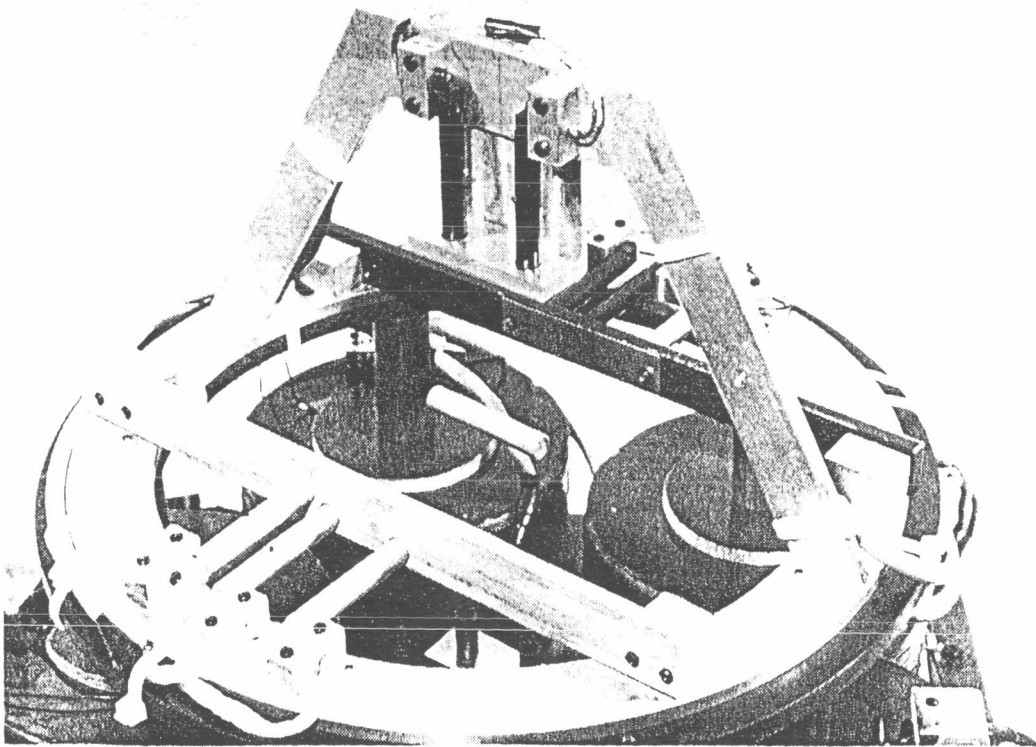
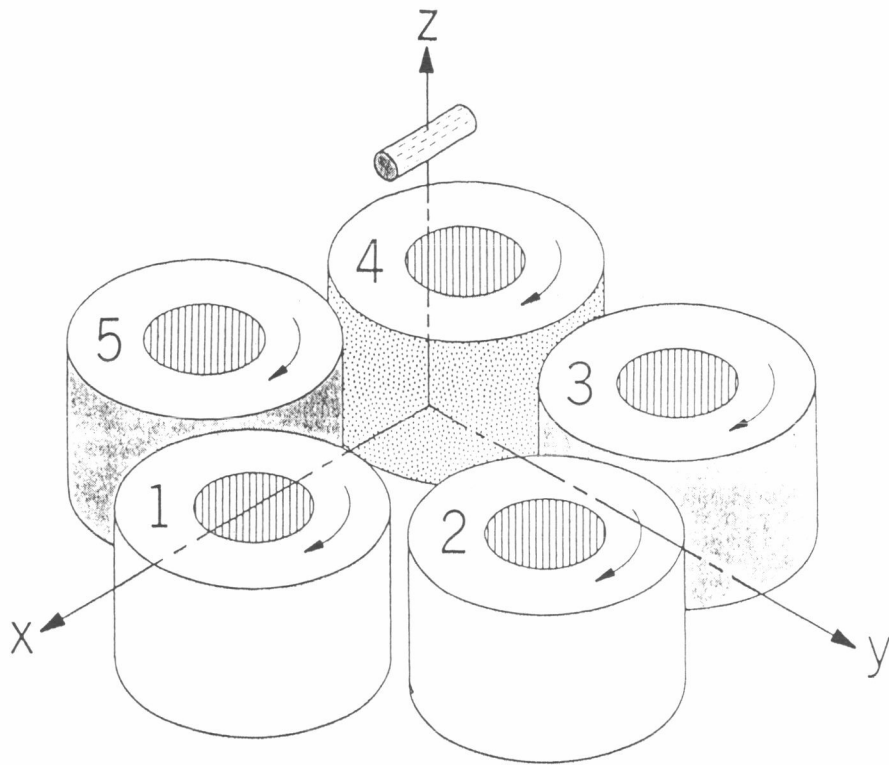
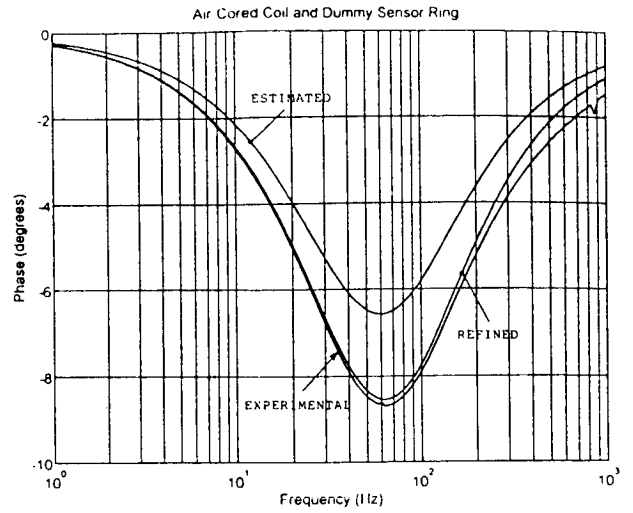
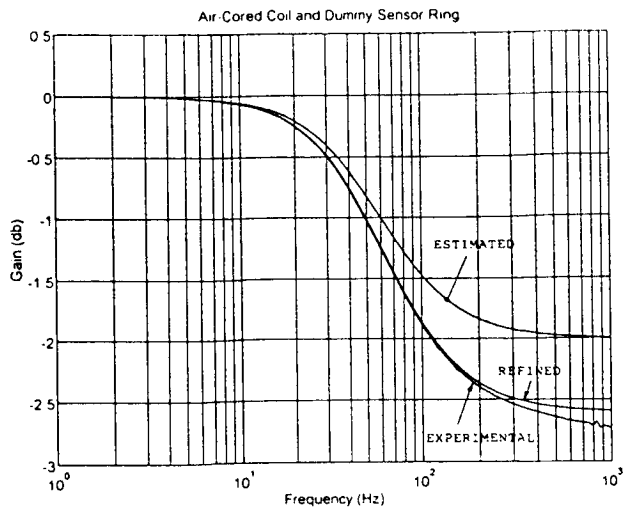
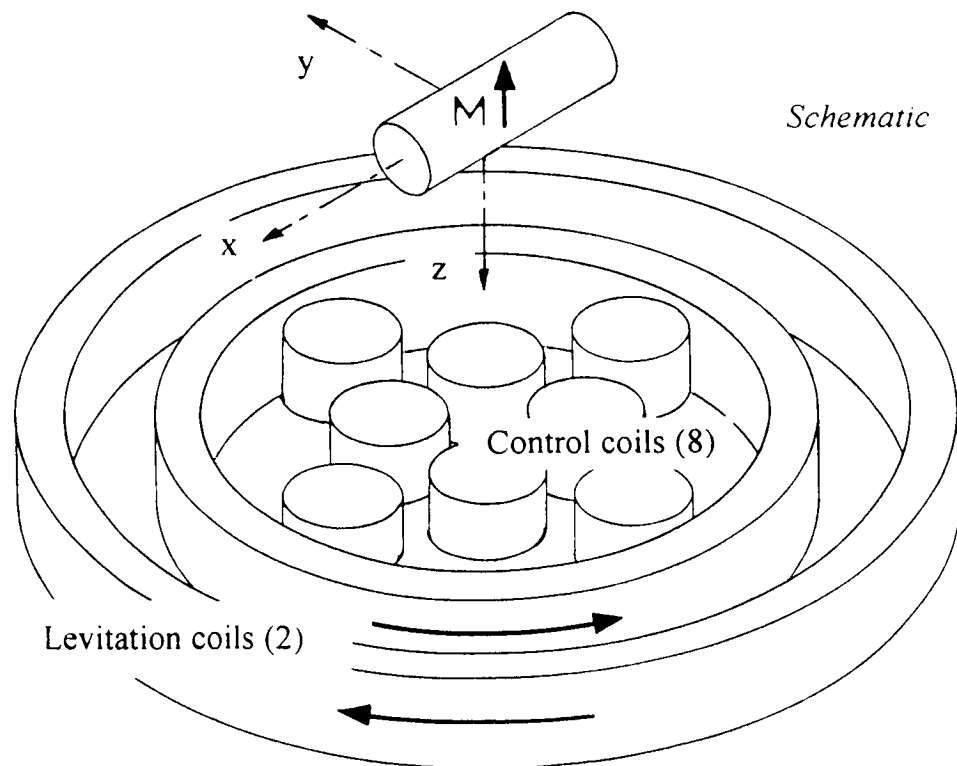


Figure 4 - The Large Angle Magnetic Suspension Test Fixture



**Figure 5 - Typical Results for Eddy Current Effects in LAMSTF**  
 Vertical field at centroid of levitated model, partial simulated sensor frame [1]



**Figure 6 - The 6DOF-8C/2L Levitation Configuration**  
 Schematic

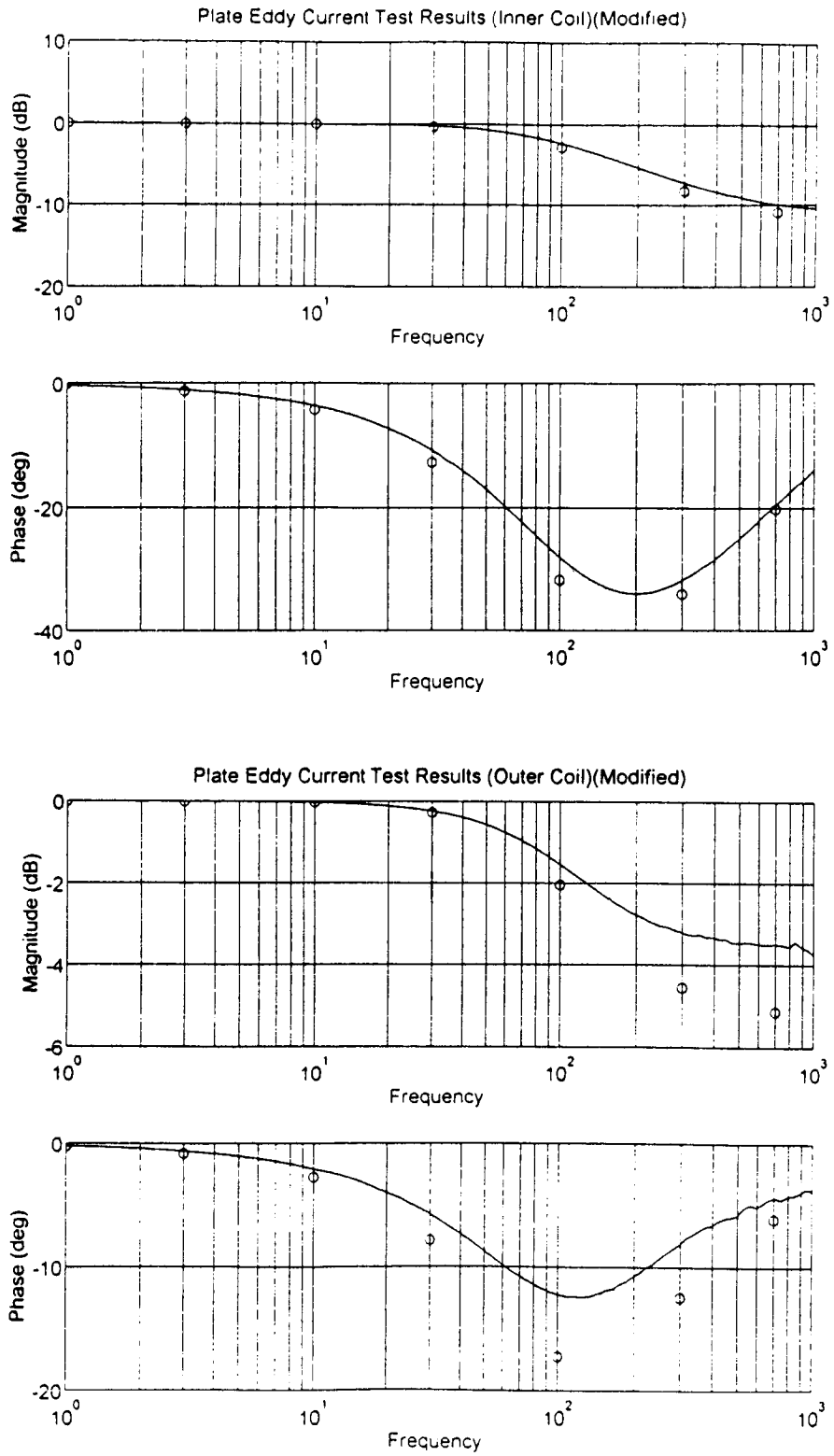
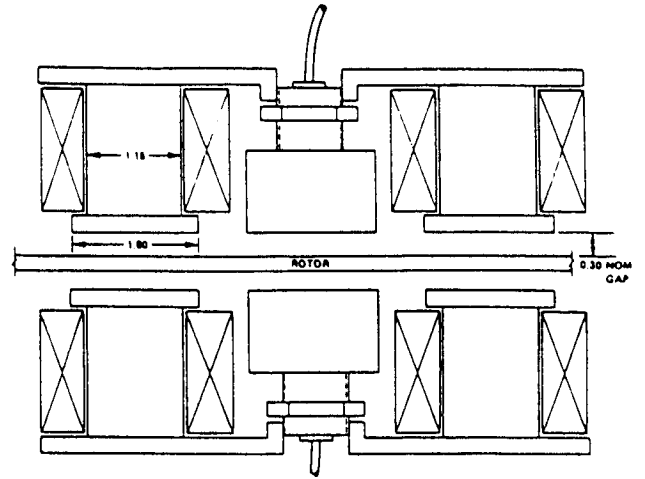
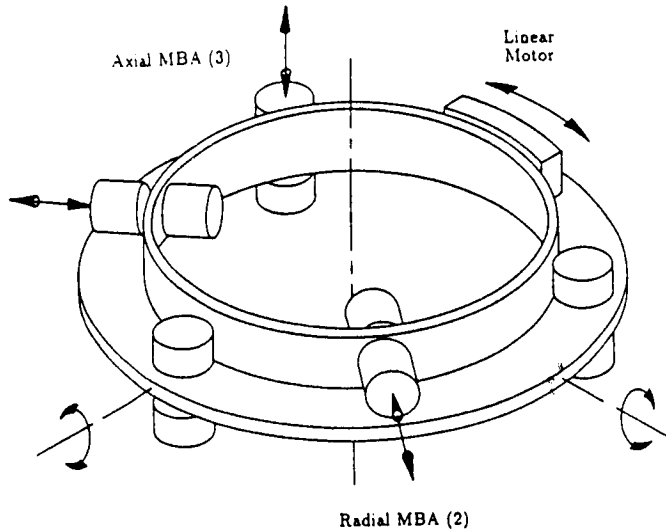


**Figure 7 - Typical Results for the 6DOF-8C/2 L System**  
 One inner control coil energized (upper graphs)  
 One outer control coil energized (lower graph)

**Figure 8 - The Annular Suspension and Pointing System Schematic**



**ASPS Axial Bearing Station (dimensions in inches)**

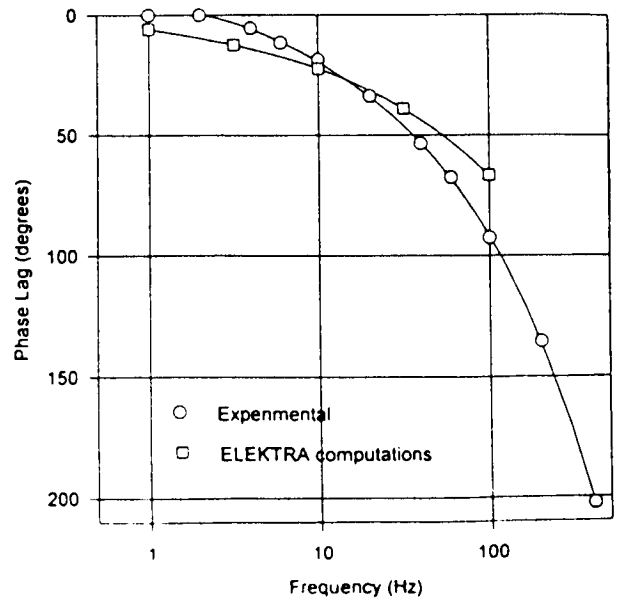
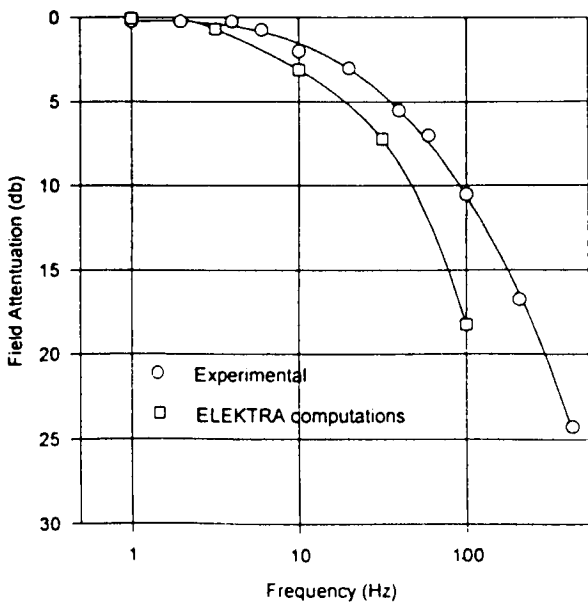


**Figure 9 - ELEKTRA Results for Air-Gap Flux**